Mem. S.A.It. Suppl. Vol. 21, 14

Memorie della
Supplementi

Probing the environment of GRBs with absorption-line spectroscopy

P. M. Vreeswijk[1] C. Ledoux[2] A. De Cia[1] A. Smette[2]

[1] Centre for Astrophysics and Cosmology, Science Institute, University of Iceland, Dunhagi 5, 107 Reykjavik, Iceland e-mail: pmv@raunvis.hi.is

[2] European Southern Observatory, Alonso de Córdova 3107, Casilla 19001, Santiago 19, Chile

Abstract. We provide a brief overview of what has been learnt about the environment of GRBs from absorption-line spectroscopy of their afterglows. In particular, we discuss measurements of the redshifts, HI and metal column densities, the molecular and dust content, and kinematics. Using the detection of absorption-line variability, it is possible to estimate the distance of the neutral absorbing material from the GRB through excitation- and ionization-modelling, which is found to be at least 100 pc away from the GRB. Finally, we examine the possibility of probing the environment closer to the GRB with high-ionization lines.

Key words. Gamma-ray burst: individual: GRB 080310 - Instrumentation: spectrographs - Galaxies: quasars: absorption lines - Galaxies: ISM - Galaxies: abundances -Radiation mechanisms: general

1. Introduction

1.1. Redshifts

Gamma-Ray Burst (GRB) afterglow spectroscopy provides a wealth of information on the interstellar medium of GRB-selected star-forming galaxies. First and foremost the crucial redshift. In the majority of cases the redshift is determined through absorption-line spectroscopy, rather than by detection of emission lines from the GRB host galaxy. We note that the emission-line method has in some cases led to a wrong redshift due to misidentification of the host. However, the absorption-line method is not infallible either, as it is typically assumed that the highest-redshift system detected is part of the host galaxy. One can only be really sure of this, if fine-structure transitions of Fe II (and probably also Si II and O I) are detected, as these have not been observed in absorbers along QSO sightlines and, moreover, the population of the Fe II excited levels has been shown to be caused by excitation by the GRB afterglow itself (see Vreeswijk et al. 2007, and Sect. 2.2).

An important conclusion of a study of an X-ray selected sample of *Swift* GRBs by Fynbo et al. (2009), is that GRBs with a redshift determination tend to have significantly lower X-ray determined total hydrogen column densities than GRBs without a redshift. Therefore, the sample of GRBs with redshifts appears to be biased toward host galaxies with less intrin-

Send offprint requests to: P. M. Vreeswijk sic extinction. The fraction of so-called dark bursts, according to the definition of Jakobsson et al. (2004), is quite large in the Fynbo et al. sample: 25%-42%, consistent with the results of both Perley et al. (2009) and Greiner et al. (2011).

1.2. H I column densities and metallicities

Even though GRBs with redshift measurements show evidence for less extinction along the sightline in the host, their typical neutral hydrogen (H I) column density as measured from the Lyα transition is formidable: on average much larger than that found in damped Lyα (DLA) systems along QSO sightlines (see Vreeswijk et al. 2004; Jakobsson et al. 2006). An interesting application to these H I column measurements, proposed by Chen et al. (2007), is to constrain the escape fraction of ionizing photons from $z > 2$ (GRB) star-forming galaxies, which was estimated to be of the order of 2% (Chen et al. 2007). Comparison of the absorption-line metallicities (using Zn II, Si II or S II transitions) measured in GRB- and QSO sightlines also suggests that GRB hosts have somewhat higher metallicities (see Prochaska et al. 2007; Savaglio et al. 2009), but this difference is not so clear as for the H I columns. Moreover, many GRB metallicities are measured from low- or medium-resolution spectra (whereas most QSO sightline metallicities are based on high-resolution data), which not only leads to large uncertainties, but could also result in the host-galaxy metallicities being underestimated (see Prochaska 2006). Ledoux et al. (2009) have measured the metallicity for several GRBs observed with the high-resolution UVES spectrograph at the VLT, and find 5 out of 6 to be below 3% compared to the solar abundance, and one at 40% solar. However, as these authors note, the high-resolution data probably suffer from the bias that only the brightest GRB afterglows, the ones with little or no dust extinction, make it into the high-resolution sample, therefore leading to lower metallicity estimates.

1.3. Dust and molecules

The evidence for a large fraction of dark bursts suggests the presence of a considerable amount of dust in at least some GRB hosts. The dust content can be crudely estimated through absorption-line spectroscopy, by comparing the abundance of an element which is typically depleted onto dust grains, such as iron, with a non-depleted element, such as zinc. GRB hosts extend the observed trend between dust depletion and zinc column density as displayed by QSO-DLAs (see figure 1 of Schady et al. 2011), and one would therefore expect GRB-DLAs to harbour more dust than their QSO-DLA counterparts. The dust content can also be estimated by assuming that any departure from the powerlaw spectrum expected from theory, is due to dust extinction. Such an analysis has now been performed for large samples, using either photometry (Kann et al. 2010; Greiner et al. 2011) or spectrophotometry (Zafar et al. 2011). Through this method the type of dust extinction can also be inferred by comparison with the few known extinction curves, mainly that of the Milky Way and the Large and Small Magellanic Clouds. Although this way of typing is often not very decisive, it is unambiguous in the few cases that the 2175 Å has clearly been detected (e.g. Elíasdóttir et al. 2009), where the extinction can be attributed to a Milky Way type of dust. Zafar et al. (2011) find that the 7% of cases for which there is strong evidence for the 2175 Å feature, the inferred extinction is rather high, suggesting that the feature may often be present but hidden from view along highly extincted sightlines.

If GRBs originate from regions of massive star formation, one would expect to regularly observe H_2 or CO molecules along the sightline. The early lack of such detections (but see Fynbo et al. 2006) led Tumlinson et al. (2007) to suggest that a combination of low metallicity and a far-ultraviolet radiation field 10-100 times than in our Galaxy, could be supressing the formation of molecular hydrogen in GRB hosts. Ledoux et al. (2009) used the high-resolution UVES GRB afterglow sample to show that the low metallicity of the sample of

GRB hosts could be solely held responsible for the lack of molecular detections. This debate was settled with the spectacular observation of series of both H_2 (including vibrationally excited H_2 Sheffer et al. 2009) and CO transitions in spectra of the roughly solar-metallicity GRB 080607 (Prochaska et al. 2009), which allowed for detailed inferences about the state of the gas, such as the (vibrationally excited) H_2 and CO column densities, doppler parameters and excitation temperature, as well as its distance from the GRB. The inferred host-galaxy extinction is quite high: A_V=3.2 mag, and shows that more molecule detections are to be expected once we delve deeper into the highly extincted population of GRB sightlines.

1.4. Kinematics - galactic outflow

High-resolution spectroscopy, with 5-10 km s^{-1} of resolution, offers the possiblity to study the gas kinematics in the GRB host galaxy. Using high-ionization lines such as O VI and C IV, Fox et al. (2008a) find evidence for a lingering tail of absorption to the blue side of the systemic velocity of several GRB hosts. Such a blue tail is also observed in absorption in the Milky Way, measured by observing background QSOs, and this can be explained through outflowing gas. This suggests that the tails seen in GRB hosts could also be the result of galactic-scale outflows. In a study of the velocity fields comparing GRB- and QSO-DLAs using mainly the low-ionization transition Si II λ 1526, Prochaska et al. (2008a) find that GRB-DLAs show systematically larger equivalent widths (EW) than QSO-DLAs, which may also point to galactic outflows.

Overall, all the characteristics discussed in this introduction suggest that GRB sightlines are probing the inner regions of high-redshift galaxies, whereas QSO sightlines are typically intersecting the outskirts (see Prochaska et al. 2008a).

2. Distance of the neutral medium from the GRB

As discussed in the introduction, with absorption-line spectroscopy of GRB afterglows we can probe the gas in the GRB host galaxy by measuring its gas column densities, metallicity, molecular and dust content and kinematics. But how far away is this gas from the GRB? Is it located in its immediate vicinity, i.e. part of the massive star-forming region where long-duration GRBs are expected to explode (e.g. MacFadyen & Woosley 1999; Fruchter et al. 2006)? Or is the neutral medium situated in the foreground in the GRB host, far away from and unrelated to the GRB's place of birth? And how much does the powerful GRB and its afterglow alter its surroundings, i.e. are the measurements discussed in the introduction representative of the host-galaxy interstellar medium before the GRB exploded?

2.1. Lower limit from the presence of Mg I

Prochaska et al. (2006) used the presence of Mg I with a similar velocity profile as other low-ionization lines in the high-resolution spectra of GRB 051111, to estimate a lower limit to the distance between the GRB and the neutral absorbing medium. Mg I, with an ionization potential of 7.6 eV - lower than that of H I - would be easily ionized if it were too close to the GRB. For a sample of bursts, a lower limit of roughly 50 pc was estimated (Prochaska et al. 2006). This is consistent with calculations of the size of the ionized region (50-100 pc) created by the ionizing radiation from the GRB progenitor star (Whalen et al. 2008).

2.2. Excited absorption-line variability

Fine-structure absorption lines, arising from excited levels just above the ground state in atoms such as C I, C II, O I, Si II and Fe II, can be used as probes of the physical conditions of the gas in which they arise (Bahcall & Wolf 1968; Silva & Viegas 2002). Vreeswijk et al. (2004) noted the presence of fine-structure lines of

Si II in afterglow spectra of GRB 030323. Although fine-structure transitions of C I and C II are commonly observed in QSO-DLAs (e.g. Wolfe et al. 2003), Si II* transitions have never been clearly detected in QSO-DLAs. They do appear in spectra of associated systems, i.e. absorbers associated with the QSO host galaxy, and have also been observed in lensed Lyman Break Galaxies (LBGs), such as MS1512-cB58 (Pettini et al. 2002), and - in emission - in a composite LBG spectrum (Shapley et al. 2003). This suggests that either the Si II atoms are excited by the GRB afterglow itself, or are due to a particular characteristic of the GRB host galaxy, such as an increased UV ambient radiation field or a higher particle density, than what is typically found in QSO-DLAs.

Even more exotic fine-structure transitions of Fe II were detected in high-resolution spectra of GRBs 050730 (Chen et al. 2005) and 051111 (Prochaska et al. 2006; Penprase et al. 2006); these are normally found only in extreme environments, such as that of η Carinae (Gull et al. 2005) and QSO associated systems (Hall et al. 2002). A comprehensive analysis by Prochaska et al. (2006) concluded that the most likely mechanism responsible for the Fe II excited-level population in GRBs 050730 and 051111 is UV pumping, but they could not rule out collisions (with free electrons) as a possible cause. This was settled by the detection of variability of the Fe II excited-level population in GRBs 020813 (Dessauges-Zavadsky et al. 2006) and 060418 (Vreeswijk et al. 2007), as shown in Fig. 1. The latter study conclusively showed that UV pumping is responsible for the evolution of the Fe II level population (Vreeswijk et al. 2007), and was able to provide an estimate of the distance between the GRB and the neutral absorbing medium of 1.7 kpc. Due to an error in equation 3 in Vreeswijk et al. (2007), however, this distance estimate was too high by a factor of $\sqrt{4\pi}$, and was recently revised down to 0.5 kpc (Vreeswijk et al. 2011b).

Since GRB 060418, time-resolved spectroscopy of other GRB afterglows - mainly using VLT/UVES combined with the Rapid-Response Mode (Vreeswijk et al. 2010) - have shown clear evidence for absorption-line variability (e.g. D'Elia et al. 2009). For other cases, variability could not clearly be established due to the limited observed time range, but thanks to the many different excited levels detected, a reliable distance estimate through UV pumping modelling could still be obtained (e.g. Ledoux et al. 2009). In Fig. 2, taken from De Cia et al. (2011), we show the GRBs for which a distance estimate could be secured. We note that all distances have been corrected for the $\sqrt{4\pi}$ factor (Vreeswijk et al. 2011b).

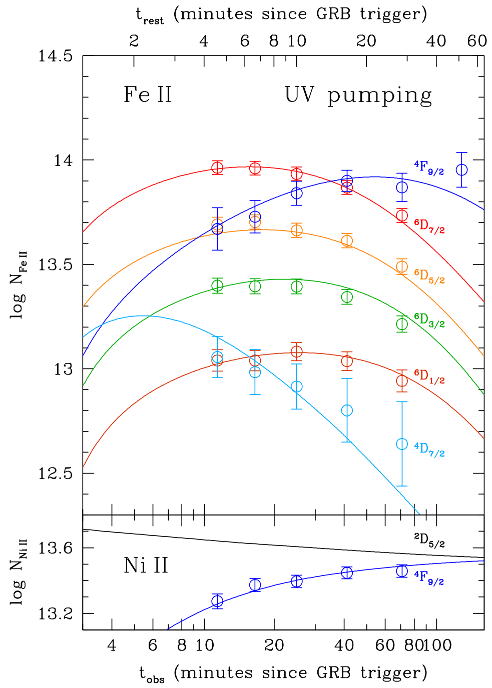

Fig. 1. The column-density evolution of Fe II (top panel) and Ni II (bottom). The open symbols denote the measurements from the VLT/UVES spectra, with different colors depicting different energy levels. The model (solid lines), in which UV photons from the flux-variable afterglow are responsible for the excited-level population as a function of time, is working remarkably well (Vreeswijk et al. 2007). The best-fit distance between the GRB and neutral absorber was initially found to be 1.7 kpc, but this has recently been revised to 0.5 kpc (Vreeswijk et al. 2011b).

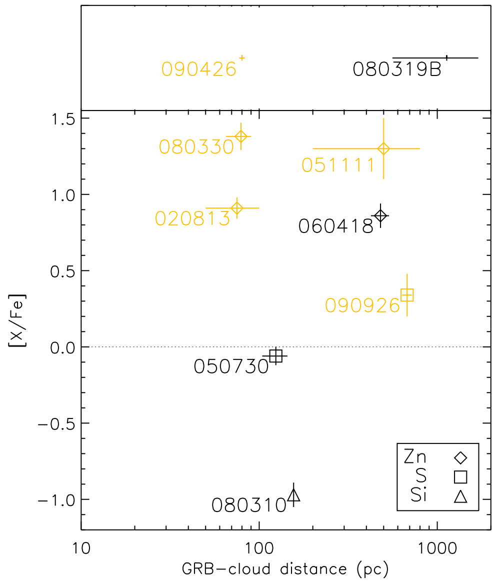

Fig. 2. The abundance ratio of zinc, sulphur or silicon over iron, compared to the GRB-absorber distance inferred from absorption-line (variability) modelling. We consider the distance estimates for the ones depicted in black more reliable, as they were observed at high spectral resolution and either show variability, or they display absorption lines from many different excited levels.

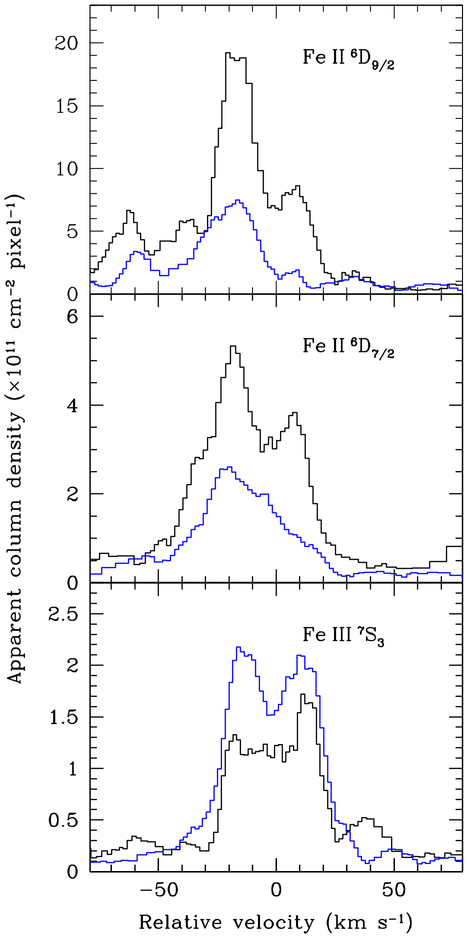

Fig. 3. Apparent column density profiles for three selected levels: Fe II ground state (top panel), the first excited level of Fe II (middle), and the 17th excited level of Fe III (bottom). The black (blue) line shows the measurements at 21 (50) minutes post-burst. It is clear that the population of the Fe II levels are decreasing in time, while Fe III shows the opposite trend (De Cia et al. 2011).

2.3. GRB 080310: excitation and ionization

Although absorption-line variability due to *ionization* of neutral material surrounding a GRB has been predicted (Perna & Loeb 1998), it has never been convincingly detected (but see Thöne et al. 2011). In a careful analysis of VLT/UVES time-resolved spectra of GRB 080310, De Cia et al. (2011) find that the population of all Fe II levels, including the ground state, is decreasing in time, as shown in Fig. 3. Moreover, these authors detect absorption from a highly-excited level of Fe III, never observed before in GRB afterglow spectra, whose population is *increasing* in time (see Fig. 3). This is highly suggestive of Fe II ionization taking place during the time interval covered by the spectra. However, the GRB host shows a very low H I column density, which could also explain the presence of Fe III, as such a low column would not shield the Fe II atoms from being ionized to Fe III by the ambient radiation field (i.e. before the occurence of the GRB explosion).

To discriminate between these two explanations, we have included ionization in our excitation program, which allows us to model the evolution of the Fe II, Fe III and H I ion col-

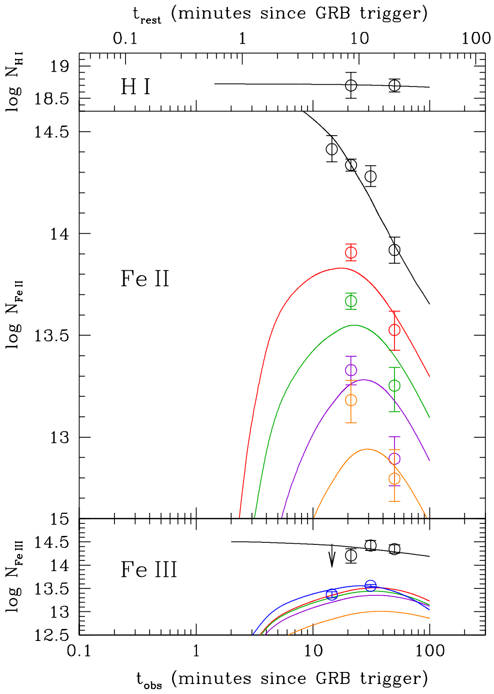

Fig. 4. The observed (total) column density evolution as a function of time, as measured for H I (top panel), Fe II (middle), and Fe III (bottom), is indicated with the open circles; an arrow indicates an upper limit. The different colours denote the different ion levels: black for the ground state, red-green-purple-orange for the first four excited levels, and with the Fe III $^7S_3$ level indicated in blue. The solid lines show the model fits. The best-fit distance with this model is about 300 pc (Vreeswijk et al. 2011a).

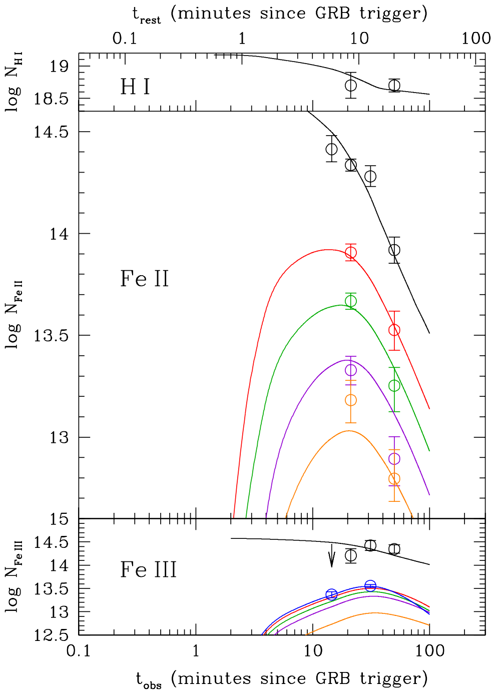

Fig. 5. Same as Fig. 4, but including an additional cloud closer to the GRB, which is ionized completely by the time of our first observations. The best-fit distance applying this model is about 150 pc (Vreeswijk et al. 2011a).

umn densities as measured by De Cia et al. (2011). We also include the H I and He I column density evolution, as these are very effective in shielding the Fe II atoms from any ionizing radiation, provided that their column densities are sufficiently large. For more details on the excitation and ionization calculations, see Vreeswijk et al. (2011a).

As can be seen in Fig. 4, the absorption-line variability can be explained by the GRB afterglow ionizing and exciting a neutral GRB absorber at a distance of roughly 300 pc away from the GRB. The very low H I column allows the Fe II ions to be ionized at this relatively large distance. Although the fit is decent, it is not very good, with a reduced chi-square of χ^2_ν=3.5. The main reason for this relatively high chi-square is the deviation of the model fit from the observed values of the Fe II fine-structure levels (the red-green-purple-orange lines in Fig. 4).

Since the Fe II excited levels are underpredicted by the model, we attempted to place an additional cloud along the line of sight, in between the GRB and the original cloud. If the additional cloud is sufficiently close to the burst, it can be completely ionized within minutes of the GRB and it would not show up in our spectra. But at the same time it would partially shield the original cloud from ionizing radiation released during the first minutes, allowing the original (observed) cloud to be closer to the burst, increasing the amount of excitation. The existence of such an additional cloud along the line of sight would not be unexpected in the gas-rich massive-star forming region in which GRBs are thought to occur. The fit with such an additional cloud, shown in Fig. 5, results in a significantly lower chi-square value ($\chi^2_\nu = 2.5$), but at the cost of three additional fit parameters. An F-test confirms the significance of the fit improvement introduced by the foreground cloud, with a null-probability of $P = 0.068$, i.e. there is a 7% chance that such improvement is random.

The relatively large population of the $^7S_3$ excited level of Fe III with respect to that of the ground state, roughly 10%, cannot be explained by excitation of Fe III ground-state ions alone. This can be seen in Fig. 6, where $^7S_3$ is easily depopulated via transitions to the $^5P^o$ term (with transition probabilities of A=10^6-10^7 s^{-1}), and then down to the $^5S_2$ level and ground term. In fact, we found that ionization of Fe II ions is required to populate the Fe III $^7S_3$ level as observed. The ground configuration of Fe II is $3d^64s$, i.e. with 6 electrons in the $3d$ shell, and a single one in the $4s$ shell. The probability of ionizing ground-state Fe II by removal of a $3d$ electron is comparable to that by removing a $4s$ electron. Quantum-mechanical calculations show that roughly 30% of all the Fe II ionizations (from the ground state) end up in the lowest level of the $3d^54s$ configuration. And this level corresponds to the excited Fe III $^7S_3$ level that is observed. This is a very strong argument that we are indeed witnessing ionization of Fe II to Fe III during the UVES observations.

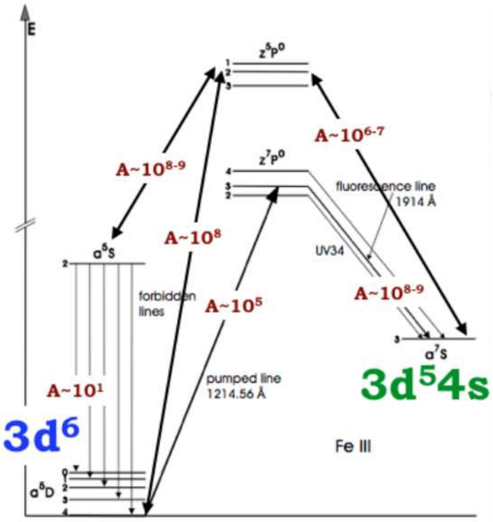

Fig. 6. Figure adapted from Johansson et al. (2000). The observed excited Fe III $^7S_3$ level is the lowest of the Fe III $3d^54s$ configuration. Although it is easily populated through excitation of ground-state ions via the $^7P^o$ term, it is also depopulated steadily via the $^5P^o$ and ^5S terms. Ionization of Fe II provides the key to explaining why the $^7S_3$ level is so heavily populated: quantum-mechanical calculations show that 30% of the ionized Fe II ends up in this level (see Vreeswijk et al. 2011a).

2.4. Do high-ionization lines probe the GRB vicinity?

Low-ionization lines seem to probe the host-galaxy ISM starting from about 100 pc away from the GRB, but possibly the high-ions will be able to take us closer. Prochaska et al. (2008b) noted that N V is detected almost always in GRB afterglow spectra, and that it displays a kinematically cold velocity profile similar to that of the Fe II fine-structure lines. These authors argue that the N V presence is due to the GRB afterglow ionizing nitrogren at distances of the order of 10 pc. Fox et al. (2008a) find that for about half of their sample of 7 GRB sightlines, the N V show a strong single component suggestive of a circumburst origin, but they cannot rule out an interstellar origin. For one case, GRB 050730, in which the N V lines show at least two components, Fox et al. (2008b) place a lower limit on the distance between the GRB and the S IV absorption from the non-detection of S IV fine-structure lines, of roughly 100 pc (see Vreeswijk et al. 2011b). If N V is indeed close to the burst, absorption-line variability is predicted (Prochaska et al. 2008b), but this has not been observed so far. Future high-resolution spectroscopy of GRB afterglows will be able to answer this question.

References

Bahcall, J. N. & Wolf, R. A. 1968, ApJ, 152, 701

Chen, H., Prochaska, J. X., Bloom, J. S., & Thompson, I. B. 2005, ApJ, 634, L25
Chen, H.-W., Prochaska, J. X., & Gnedin, N. Y. 2007, ApJ, 667, L125
De Cia, A., et al. 2011, A&A, submitted
D'Elia, V., et al. 2009, ApJ, 694, 332
Dessauges-Zavadsky, M., et al. 2006, ApJ, 648, L89
Elíasdóttir, Á., et al. 2009, ApJ, 697, 1725
Fox, A. J., et al. 2008a, A&A, 491, 189
Fox, A. J., et al. 2008b, A&A, 491, 189
Fruchter, A. S., et al. 2006, Nature, 441, 463
Fynbo, J. P. U., et al. 2009, ApJS, 185, 526
Fynbo, J. P. U., et al. 2006, A&A, 451, L47
Greiner, J., et al. 2011, A&A, 526, A30+
Gull, T. R., et al. 2005, ApJ, 620, 442
Hall, P. B., et al. 2002, ApJS, 141, 267
Jakobsson, P., et al. 2006, A&A, 460, L13
Jakobsson, P., et al. 2004, ApJ, 617, L21
Johansson, S., et al. 2000, A&A, 361, 977
Kann, D. A., et al. 2010, ApJ, 720, 1513
Ledoux, C., et al. 2009, A&A, 506, 661
MacFadyen, A. I. & Woosley, S. E. 1999, ApJ, 524, 262
Penprase, B. E., et al. 2006, ApJ, 646, 358
Perley, D. A., et al. 2009, AJ, 138, 1690
Perna, R. & Loeb, A. 1998, ApJ, 501, 467
Pettini, M., et al. 2002, ApJ, 569, 742
Prochaska, J. X. 2006, ApJ, 650, 272
Prochaska, J. X., Chen, H.-W., & Bloom, J. S. 2006, ApJ, 648, 95
Prochaska, J. X., Chen, H.-W., Dessauges-Zavadsky, M., & Bloom, J. S. 2007, ApJ, 666, 267
Prochaska, J. X., et al. 2008a, ApJ, 672, 59
Prochaska, J. X., Dessauges-Zavadsky, M., Ramirez-Ruiz, E., & Chen, H.-W. 2008b, ApJ, 685, 344
Prochaska, J. X., et al. 2009, ApJ, 691, L27
Savaglio, S., Glazebrook, K., & Le Borgne, D. 2009, ApJ, 691, 182
Schady, P., et al. 2011, A&A, 525, A113+
Shapley, A. E., Steidel, C. C., Pettini, M., & Adelberger, K. L. 2003, ApJ, 588, 65
Sheffer, Y., et al. 2009, ApJ, 701, L63
Silva, A. I. & Viegas, S. M. 2002, MNRAS, 329, 135
Thöne, C. C., et al. 2011, MNRAS, 414, 479
Tumlinson, J., Prochaska, J. X., Chen, H.-W., Dessauges-Zavadsky, M., & Bloom, J. S. 2007, ApJ, 668, 667
Vreeswijk, P. M., et al. 2004, A&A, 419, 927
Vreeswijk, P. M., Kaufer, A., Spyromilio, J., et al. 2010, in Society of Photo-Optical Instrumentation Engineers (SPIE) Conference Series, Vol. 7737, Society of Photo-Optical Instrumentation Engineers (SPIE) Conference Series
Vreeswijk, P. M., et al. 2011a, A&A, submitted
Vreeswijk, P. M., et al. 2007, A&A, 468, 83
Vreeswijk, P. M., et al. 2011b, A&A, 532, C3+
Whalen, D., Prochaska, J. X., Heger, A., & Tumlinson, J. 2008, ApJ, 682, 1114
Wolfe, A. M., Prochaska, J. X., & Gawiser, E. 2003, ApJ, 593, 215
Zafar, T., et al. 2011, ApJ, 735, 2